

Segmentation of the heart and great vessels in CT images using Curvelet Transform and Multi Structure Elements Morphology

S. Josevin Prem, M.S Ulaganathan, G. Kharmega Sundararaj

Abstract—A new method for heart vessel segmentation is proposed. Regarding the high ability of FDCT in representing images containing edges, using modification of curvelet transform coefficients, the image contrast was improved and prepared better for segmentation step. Due to high sensitivity of multi structure elements to edges in all directions, multi structure elements morphology was capable of detecting the blood vessel edges successfully. Morphological opening by reconstruction using multi structure elements removed the false edges, while preserved the thin vessel edges perfectly. By applying the CCA and length filtering locally, benefited from adaptive processing and it helped to remove the remained false edges more accurately. The heart blood vessel image contrast was improved and prepared better for segmentation step. The results of both segmentation and enhancement steps show that our method effectively detects the blood vessels with accuracy of above 94% in less than 1 min.

Keywords: Heart segmentation, Model-based segmentation Shape variability, Computed tomography.

I. INTRODUCTION

Imaging is a basic aspect of medical sciences for visualization of anatomical structures and functional or metabolic information of the human body [1]. Structural and functional imaging of human body is important for understanding the human body anatomy, physiological processes, function of organs, and behavior of whole or a part of organ under the influence of abnormal physiological conditions or a disease [2,3]. For the last two decades, radiological sciences have witnessed a revolutionary progress in medical imaging and computerized medical image processing, some important radiological tools in diagnosis and treatment evaluation and intervention of critical diseases have much significant improvement for health care. So, medical imaging in diagnostic radiology is evolving as a result of the significant contributions of a number of different disciplines from basic sciences, engineering, and medicine. Therefore, computerized image reconstruction, processing and analysis methods have been developed Magnetic resonance (MR) imaging has several advantages over other medical imaging modalities, including high contrast among different soft tissues, relatively high spatial resolution across the entire field of view and multi-spectral characteristics Cardiac computed tomography (CT) is an important imaging modality for diagnosing cardiovascular disease and it can provide detailed anatomic information about the cardiac chambers, large vessels or coronary arteries. Segmentation of cardiac chambers is a prerequisite for quantitative functional analysis and various approaches have

been proposed in the literature [6, 7]. Except for a few works [5, 24], most of the previous research focuses on the left ventricle (LV) segmentation. However, complete segmentation of all four heart chambers, as shown in Fig. 1, can help to diagnose diseases in other chambers, e.g., left atrium (LA) fibrillation, right ventricle (RV) overload or to perform dis-synchrony analysis.

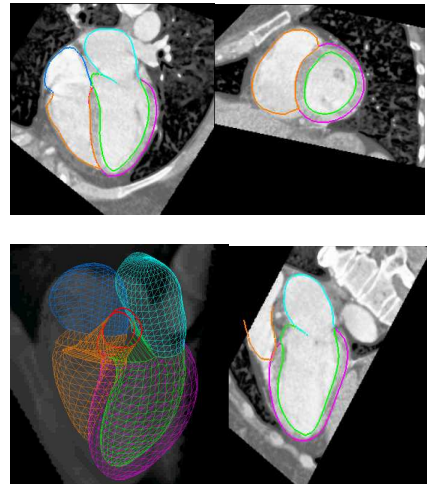


Fig. 1. Complete segmentation of all four chambers in a CT volume with green for the left ventricle (LV) endocardial surface, magenta for LV epicardial surface, cyan for the left atrium (LA), brown for the right ventricle (RV), and blue for the right atrium (RA).

Cardiac computed tomography (CT) is an important imaging modality for diagnosing cardiovascular disease and it can provide detailed anatomic information about the cardiac chambers, large vessels or coronary arteries. Segmentation of cardiac chambers is a prerequisite for quantitative functional analysis and various approaches have been proposed in the literature.1, 2 Except for a few instances,3, 4 most of the previous research focuses on the left ventricle (LV) segmentation. However, complete segmentation of all four heart chambers, as shown in Fig. 1, can help to diagnose diseases in other chambers, e.g., left atrium (LA) fibrillation, right ventricle (RV) overload or to perform dyssynchrony analysis. There are two major tasks to develop an automatic segmentation system: heart modeling (shape representation) and automatic model fitting (detection or segmentation). These two tasks are closely related different.

There are two tasks for a non-rigid object segmentation problem: object localization and boundary delineation. Most of the previous approaches focus on boundary de- lineation

based on active shape models (ASM) [22], active appearance models (AAM) [1, 13], and deformable models [2, 4, 5, 8, 12, 17]. There are a few limitations inherent in these techniques: 1) Most of them are semiautomatic and manual labeling of a rough position and pose of the heart chambers is needed. 2) They are likely to get stuck in local strong image evidence. Other techniques are straightforward extensions of 2D image segmentation to 3D [10, 18, and 25]. The segmentation is performed on each 2D slice and the results are combined to get the final 3D segmentation. However, such techniques cannot fully exploit the benefit of 3D imaging in a natural way. Lorenzo-Valde's et al. [11] proposed a registration based approach, but its performance is not clear for large datasets.

Object localization is required for an automatic segmentation system and discriminative learning approaches have proved to be efficient and robust for solving 2D problems. In these methods, shape detection or localization is formulated as a classification problem: whether an image block contains the target shape or not [16, 23]. To build a robust system, a classifier only has to tolerate limited variation in object pose. The object is found by scanning the classifier over an exhaustive range of possible locations, orientations, scales or other parameters in an image. This searching strategy is different from other parameter estimation approaches, such as deformable models, where an initial estimate is adjusted (e.g., using the gradient descent technique) to optimize a predefined objective function.

Exhaustive searching makes the system robust under local minima, however there are two challenges to extend the learning based approaches to 3D. First, the number of hypotheses increases exponentially with respect to the dimensionality of the parameter space. For example, there are nine degrees of freedom for the anisotropic similarity transformation¹, namely three translation parameters, three rotation angles, and three scales. Suppose we search n discrete values for each dimension, the number of tested hypotheses is n^9 (for a very coarse estimation with a small $n=5$, $n^9 = 1,953,125$). The computational demands are beyond the capabilities of current desktop computers. Due to this limitation, previous approaches often constrain the search to a lower dimensional space. For example, only the position and isotropic scaling (4D) is searched in the generalized Hough transformation based approach [19]. Hong et al. [9] extended the learning based approach to a 5D parameter space for semi-automatic segmentation. The second challenge is that we need efficient features to search the orientation and scale spaces. Haar wavelet features can be efficiently computed for translation and scale transformations [15, 23]. However when searching for rotation parameters one either has to rotate the feature templates or rotate the volume which is very time consuming. The efficiency of image feature computation becomes more important when combined with a very large number of test hypotheses.

II. HEART SEGMENTATION

Given a heart chamber model, we need to develop a scheme to fit the model onto an input volume automatically.

Since the heart is a non-rigid shape, the model fitting (or heart chamber segmentation) procedure can be divided into two steps: object localization and boundary delineation. Most of the previous approaches focus on boundary delineation based on active shape models (ASM), 5 active appearance models (AAM), 6, 7 and deformable models.³, 8–12. There are a few limitations inherent in these techniques: 1) Most of them are semi-automatic and manual labeling of a rough position and pose of the heart chambers is needed. 2) They are likely to get stuck in local strong image evidence. Other techniques are straightforward extensions of 2D image segmentation to 3D.^{17–19} The segmentation is performed on each 2D slice and the results are combined to get the final 3D segmentation. However, such techniques cannot fully exploit the benefit of 3D imaging in a natural way. LorenzoVald'es et al.²⁰ proposed a registration based approach, but its performance is not clear for large datasets.

Object localization is required for an automatic segmentation system and discriminative learning approaches have proved to be efficient and robust for solving 2D problems. In these methods, shape detection or localization is formulated as a classification problem: whether an image block contains the target shape or not.²¹ To build a robust system, a classifier only has to tolerate limited variation in object pose. The object is found by scanning the classifier exhaustively over a range of possible locations, orientations, scales or other parameters in an image. This searching strategy is different from other parameter estimation approaches, such as deformable models, where an initial estimate is adjusted (e.g., using the gradient descent technique) to optimize a predefined objective function.

Exhaustive searching makes the system robust under local minima. However, there are two challenges to extend the learning based approaches to 3D. First, the number of hypotheses increases exponentially with respect to the dimensionality of the parameter space. For example, there are nine degrees of freedom for the anisotropic similarity transformation[†], namely three translation parameters, three rotation angles, and three scales. Suppose we search n discrete values for each dimension, the number of tested hypotheses is n^9 (for a very coarse estimation with a small $n=5$, $n^9 = 1,953,125$). The computational demands are beyond the capabilities of current desktop computers. Due to this limitation, previous approaches often constrain the search to a lower dimensional space. For example, only the position and isotropic scaling (4D) is searched in the generalized Hough transformation based approach.²² Hong et al.¹⁶ extended the learning based approach to a 5D parameter space for semi-automatic segmentation. The second challenge is that we need efficient features to search the orientation and scale spaces. Haar wavelet features can be efficiently computed under translation and scaling.²¹ However, to search for rotation parameters, one either has to rotate the feature templates or rotate the volume (the latter is time consuming). The efficiency of image feature

computation becomes more important when combined with a huge number of test hypotheses.

III. HEART AND VESSEL MODEL

We start by providing information about the image data that have been used to build the heart and vessel model. Then we present the heart and vessel model itself. We describe how the model geometry has been generated. For adapting the model to images it is important to have a parametric description of its shape variability. For that purpose we extend the description of shape variability by multiple linear transformations and show how it can be used to model bending and diameter variations of large vessels. Finally, information for boundary detection during model adaptation is attached to each triangle. In this context, we rely on the concept of Simulated Search.

A. Image data for model building

Altogether, 35 data sets from 20 patients were used for model building. The data sets were retrospectively reconstructed at various phases of the cardiac cycle. They represent typical images that can be expected in clinical routine for patients indicated for cardiac CTA. The images were acquired with 16-, 40-, and 64-slice CT scanners (Brilliance CT, Philips Healthcare, Cleveland, OH) and standard CTA protocols with in-plane voxel resolution between 0.30 to 0.30 and 0.78 to 0.78 mm² (typically 0.49 to 0.49 mm²), spacing between the slices between 0.4 to 2.0 mm (typically 0.4–0.5 mm) and slice thickness varying from 0.6 to 3.0 mm (typically twice the spacing between slices). The data sets comprise the 28 data sets of Ecabert et al. (2008) and 7 additional data sets that were particularly suited to construct the mesh geometry of the great vessels.

B. Mesh model

A geometric mesh model of the heart and the major vessels can be generated in various ways. Starting with an annotation of the different structures in an image, the mesh could be constructed from scratch. For us it was, however, important to re-use previously generated ground truth annotations and corresponding reference meshes. In addition, we wanted to have the meshes of the vessels made of regular rings as this facilitates definition of the shape variability. Hence, we used the 4-chamber heart model (Fig. 1) of Lorenz and von Berg (2006) and Ecabert et al. (2008) as starting point. This model consists of $V = 7286$ vertices combined in $T = 14,771$ triangles and represents the average heart shape of the 28 data sets used to build the model. We extended this model by generating and attaching structured meshes of the great vessels.

For that purpose, 7 CTA data sets were used in which the desired vessels were properly contrasted. These data sets also include the aortic arch and substantial portions of the superior and inferior vena cava. The centerlines of the aorta, the superior vena cava, the inferior vena cava, the coronary sinus, and the four pulmonary veins (up to the first bifurcation) were interactively delineated in these data sets and represented by equidistantly distributed points. the

epicardium around the left ventricle, the left ventricle together with the aortic trunk, and the right ventricle together with the trunk of the pulmonary artery. For the attached vessels, we combine between 3 and 6 successive structured rings into short tubular segments. To each segment, we assign an individual similarity transformation. Between two tubular segments, there is a transition region (7 mm for the aorta and 5 mm for the other vessels) to preserve a smooth mesh geometry. Fig. 3 shows the heart model with the different tubular segments represented in different colors. The description of shape variability by linear transformations assigned to model subparts is a simple and intuitive approach, though subdivision of the model is done manually. In the context of our application it has several advantages. First, shape variations of the heart chambers as well as bending and diameter variations of the vessels can be described in a single, consistent framework. Second, since shape variability is described by an empirical parameterization and not derived by statistical analysis, 7 data sets are sufficient.

To define geometry and shape variability of the great vessels. Third, parameter variations have by construction only a local influence. That is, when changing the diameter of the descending aorta, the heart chambers are not influenced. This is a difference to approaches based on principal component analysis where modification of a single parameter usually influences all parts of the model.

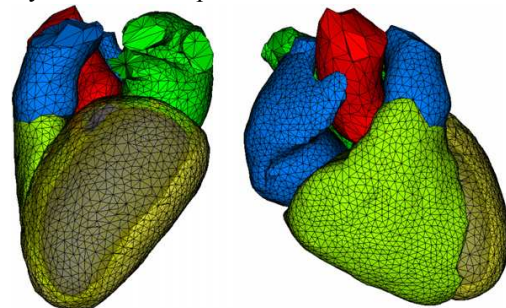


Fig. 2. 4-chamber heart model. The surface describes the endocardium except for the left ventricle where the epicardial wall is also modeled. The colors show the subdivision into different anatomical regions (epicardium of the left ventricle (yellow), endocardium of the left ventricle (gray), right ventricle (light green), left atrium (green), right atrium (light blue), aorta (red), trunk of the pulmonary artery (light blue)).

C. Adaptation of the great vessels

Adaptation of the great vessels assumes that an initial segmentation of the heart chambers is available. Afterwards the tubular segments are successively initialized, activated, and adapted. This approach allows to properly initializing the tubular segments for deformable adaptation except for the case when the aortic arch is not in the field-of-view. For that reason, a dedicated localization algorithm for the descending aorta has been introduced.

The descending aorta is localized within an axial slice that is determined from the most distal tubular segment of the descending aorta after positioning the heart model and optimizing its global orientation and scaling. Localization is done with a modified 2D Hough transformation (Hough,

1962) for circles. Candidate edges are detected using 3D methods and additional criteria are applied to reduce the number of candidates. For instance, a candidate edge is only considered, if its 3D gradient is sufficiently parallel to the axial plane (i.e. the angle between the 3D gradient vector and the axial plane should be smaller than 26.6 deg). In addition, edges with gradient magnitude or gray-value difference outside predefined ranges are skipped. During accumulation, the homogeneity within the associated circle is taken into account. To ensure that circular arcs are suppressed and only almost complete circular structures are detected, the circle is subdivided into 4 wedges and the associated counts are accumulated separately. The final vote is obtained by multiplying the results of four wedges building a circle and the circle with the maximum final vote represents the localization result for the descending aorta. 3.2.2. Adaptation of tubular segments

During deformable adaptation, the set V of active vertices consists of the vertices of the heart structures and tubular segments that are currently being adapted (i.e., these vertices belong to a triangle out of the set S for which boundary detection is performed) and of the vertices building the directly connected tubular segments.

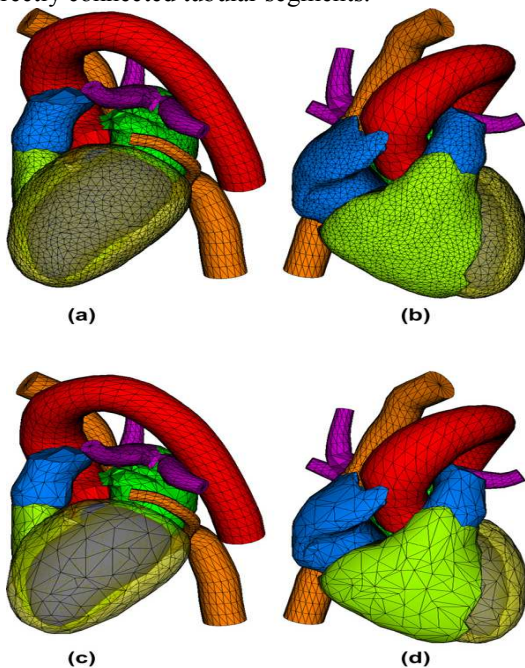


Fig 3. Heart model with the great vessels ((a and b): fine resolution; (c and d): low resolution). As for the 4-chamber heart model, the surface describes the endocardium except for the left ventricle where the epicardial wall is also modeled. The tubular structures describe the vessel lumen (aorta (red), pulmonary veins (purple), coronary sinus (orange), and inferior & superior vena cava (orange)) and are composed of regularly triangulated rings. For the low resolution mesh model only the chambers are sub-sampled.

The weights $w_{i,k}$ of the multi-linear transformation T multi-linear are defined in a way that respective tubular segments use the same transformation as the mesh part they are connected to With this mechanism, the shape of these tubular segments is defined by the internal energy and their

orientation is defined via the transformation T multi-linear. This mechanism ensures a smooth transition between mesh parts that are currently being adapted and the directly connected tubular segments, for which deformable adaptation can be activated in a subsequent iteration. In order to activate the adaptation of a tubular segment, boundary detection is enabled by adding its triangles to the set S and the multi-linear transformation T multi-linear is complemented by the transformation describing its shape variability. If a further inactive tubular segment is connected, its vertices are added to the set V of active vertices and the weights $w_{i,k}$ are defined in a way that both tubular segments use the same transformation.

VI. PROPOSED TECHNOLOGY

In this paper, a method based on using curvelet transform is proposed to enhance and prepare the image for better vessel detection. Curvelet is a new multi scale transform that is used to overcome the existing drawback of the classical multi resolution approaches such as wavelets. It can represent the edges along curves much more efficiently than the traditional wavelet. We used the second generation of curvelet transform, discrete curvelet transform (DCT), and modified the DCT coefficients by a suitable nonlinear function. One way to increase the image contrast is to enhance the image ridges, which play an important role in enhancing image contrast. In order to simultaneously enhance the weak edges and eliminate the noise, the modifying function parameters are defined based on some statistic features of fast DCT (FDCT) coefficients. The directionality feature of the multistructure elements method makes it an effective tool in edge detection. Therefore, in the following step, mathematical morphology using multistructure elements are applied to obtain the image ridges. Then, morphological opening by reconstruction helps to remove the detected ridges not belonging to the vessel tree while preserving the thin vessel edges. The morphological opening by reconstruction benefits from using multistructure elements, which helps to improve the performance of this step. There is a restriction on size of structure elements (SEs) concerning the blood vessels diameter. Therefore, the remaining false edges will be removed by means of connected components analysis (CCA) along with length filtering. In order to act locally, image is decomposed to several tiles and CCA, and length filtering is individually applied to each tile. In the enhanced images, some unrecognized thin vessels became easily recognizable and as mentioned earlier, use of statistic features of the coefficients in the enhancement function allows us to make the function more adaptive to the input image and helps us to deal with noise as it prevents the noise amplification as well. As it is shown, function parameter selection affects the result of enhancement. The aim of enhancement step is enhancing the thin vessels having low contrast to detect better in the edge detection step; however, an improper contrast enhancement may magnify the unevenness of background illumination, which cause some false edges in the edge detection step. In other words, the enhancement function enhances all weak edges in the image, which means that the edges of thin vessel and the weak edges arising from uneven background

illumination are enhanced coincidentally. To overcome this problem, an estimated image background will be subtracted from the enhanced image to decrease the roughness and those weak edges from the image. The proposed method for classification tasks based on morphological hat Scale spaces, combined with unsupervised cluster analysis, which can be used for both contour and ornamentation (texture) feature extraction. The sets of feature vectors were used in two classification experiments, using decision trees with bagging. The advantages of using the proposed hat scale-space representations are: (i) a small number of scale space entries, compared with the number of peak components; (ii) all the extracted scales are important because major changes in the topology of the signal occur at these scales; (iii) once some entries in the scale space are obtained, they can be characterized by computing not only shape and size features, but also features related to the 'height' of each peak component. In this representation, one can access and utilize linking between components at sequential grey levels in the signal.

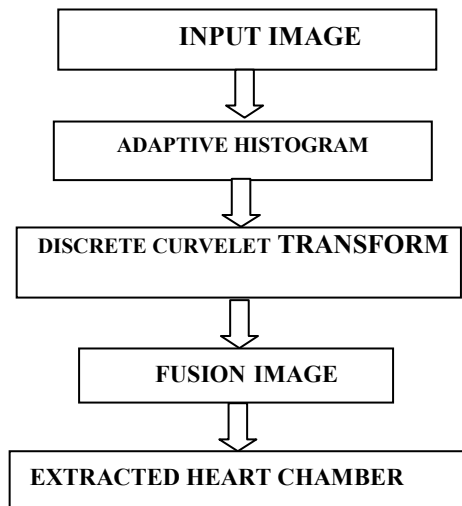


Fig. 4. Proposed Flow Diagram

An important advantage of the 1-D hat scale spaces (used on the curvature signal) as compared to the CSS method, is that the extracted features (maximum heights of the peaks of the signal) are not localized along the contour. The descriptors extracted from the CSS representation explicitly use positions along the contour, which means that they are not readily invariant under planar rotation and mirroring, and this result in additional computational overhead needed to match two shapes by the corresponding sets of descriptors. Also, all convex objects are identical for the CSS set of descriptors, since it is based on inflection points, and there are none on the contour of a convex object.

A. Gray and Color Image Contrast Enhancement by the Curvelet Transform

A new method for contrast enhancement based on the curvelet transform is proposed. The curvelet transform represents edges better than wavelets, and is therefore well-suited for multi scale edge enhancement. Contrast enhancement is used to enhance all the weak edges. This approach is compared with enhancement based on the wavelet

transform, and the Multi scale Retinex. The Multiscale Retinex (MSR) combines several SSR outputs to produce a single output image which has both good dynamic range compression and color constancy. The Multiscale Retinex introduces the concept of multi resolution for contrast enhancement. It performs dynamic range compression and can be used for different image processing goals. MSR softens the strongest edges and keeps the faint edges almost untouched. The opposite approach was proposed by Velde in using the wavelet transform for enhancing the faintest edges and keeping untouched the strongest. The strategies are different, but both methods allow the user to see details which were hardly distinguishable in the original image, by reducing the ratio of strong features to faint features.

In a range of examples, edge detection and segmentation, are used among other processing applications, to provide for quantitative comparative evaluation. The findings are that curvelet based enhancement out-performs other enhancement methods on noisy images, but on noiseless or near noiseless images curvelet based enhancement is not remarkably better than wavelet based enhancement.

B. Edge Detection & Reconstruction

In order to perform edge detection using multistructure elements morphology, the earlier SE of morphological edge detector should be replaced by new introduced SE and follow the following algorithm.

- 1) Produce the proposed SEs S_i with regard to the required directional resolution.
- 2) Apply the selected edge detector function F on the original image using the achieved SEs in 1 and get the sub edge image $F(I)_i$.
- 3) Put the $F(I)_i$ obtained in the following equation to achieve the whole of detected edges:

$$F(I) = \sum_{i=0}^{M-1} w_i F(I)_i$$

Where $F(I)$ is the total edge image, $M = 180/\alpha$ is the number of S_i and w_i is the assigned weight to each of sub edge image. In order to have the same effect of each $F(I)_i$, the assigned weights can be defined as $w_i = 1/M$, or they can be calculated by other methods as well. Also, if any information about the processed image exists, the weights can be assigned according to the degree of importance of information that may exist in each of $F(I)_i$.

C. Optimization of Length filtering

A simple method to eliminate these undesired objects is using morphological opening. Opening by reconstruction includes two steps: conventional morphological opening and reconstruction by dilation. Since the multi structure elements are highly sensitive to edges in all directions, it helps to accurately eliminate the false edges. The SE used in this step is the same as in the edge detection step. Therefore, some of undesired objects remain inevitable, which will be removed in length filtering step. In this case, the concept of CCA is used where connected components pixels which are identified above a specific threshold and labeled using eight connected neighborhood and are considered as a single object.

Considering the entire image in CCA and length filtering leads to inferior results. The thresholding equation relates to standard deviation of gray levels; therefore, the large range of gray levels may cause that considering a single threshold for the entire image lead to loss of some parts of thin vessels. In order to deal with this problem, we perform a kind of adaptive CCA, meaning that we consider images in separate tiles and apply CCA and length filtering to each tile, individually. By this means, there is no large range of gray levels in each block, and a proper threshold can be chosen which separates the false edges from vessel edges efficiently. After applying CCA, the components having length less than a specific threshold will be eliminated.

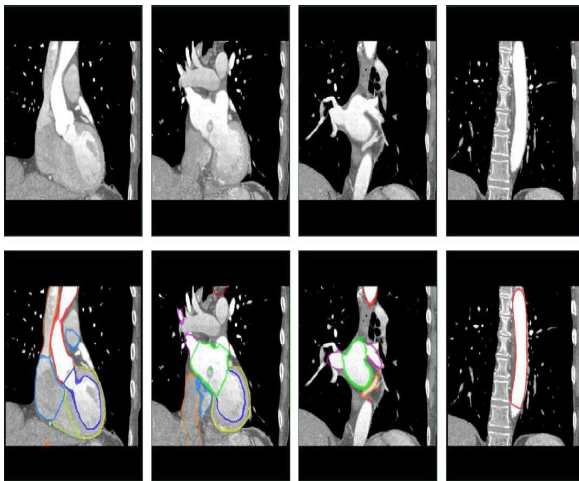


Fig. 5. Segmentation results for the heart model with the great vessels

V. SUMMARY AND CONCLUSION

An automatic model-based approach for the segmentation of the whole heart and the attached great vessels is presented. A major contribution of this article is the adaptation of a geometric model combining structurally different parts, such as rounded cardiac chambers and elongated vessels, using a single and consistent framework. The shape variability is described by an empirical parameterization and defined using a multi-linear transformation. In particular, each chamber is assigned an affine transformation whereas the great vessels are represented by the concatenation of short tubular segments, each of them undergoing a similarity transformation. This representation enables the consistent description of inter-phase and inter-patient chamber variations, and appropriate bending of the vessels.

The adaptation of this model to an image is controlled by a flexible engine which uses different techniques such as GHT-based detection, parametric model adaptation and deformable model adaptation, and schedules when and how the different parts of the model are adapted. The adaptation engine can also control the mesh resolution and the number of iterations needed for each part of the models separately. An efficient and accurate segmentation can be achieved by dynamically activating and freezing the different parts of the model.

REFERENCES

- [1] P. Schoenhagen, S.S. Halliburton, A.E. Stillman, and R.D. White, "CT of the heart: Principles, advances, clinical uses," *Cleveland Clinic Journal of Medicine*, vol. 72, no. 2, pp. 127–138, 2005.
- [2] A.F. Frangi, W.J. Niessen, and M.A. Viergever, "Three-dimensional modeling for functional analysis of cardiac images: A review," *IEEE Trans. Medical Imaging*, vol. 20, no. 1, pp. 2–25, 2001.
- [3] A.F. Frangi, D. Rueckert, and J.S. Duncan, "Three-dimensional cardio-vascular image analysis," *IEEE Trans. Medical Imaging*, vol. 21, no. 9, pp. 1005–1010, 2002.
- [4] J. Lötjönen, S. Kivistö, J. Koikkalainen, D. Smutek, and K. Lauerma, "Statistical shape model of atria, ventricles and epicardium from short- and long-axis MR images," *Medical Image Analysis*, vol. 8, no. 3, pp. 371–386, 2004.
- [5] W. Hong, B. Georgescu, X.S. Zhou, S. Krishnan, Y. Ma, and D. Comaniciu, "Database-guided simultaneous multi-slice 3D segmentation for volumetric data," in *Proc. European Conf. Computer Vision*, 2006, pp. 397–409.
- [6] D. Fritz, D. Rinck, R. Dillmann, and M. Scheuring, "Segmentation of the left and right cardiac ventricle using a combined bi-temporal statistical model," in *Proc. of SPIE Medical Imaging*, 2006, pp. 605–614.
- [7] R. Ionasec, B. Georgescu, E. Gassner, S. Vogt, O. Kutter, M. Scheuring, N. Navab, and D. Comaniciu, "Dynamic model-driven quantitative and visual evaluation of the aortic valve from 4D CT," in *Proc. Int'l Conf. Medical Image Computing and Computer Assisted Intervention*, 2008.
- [8] T.F. Cootes, C.J. Taylor, D.H. Cooper, and J. Graham, "Active shape models—their training and application," *Computer Vision and Image Understanding*, vol. 61, no. 1, pp. 38–59, 1995.
- [9] D. Fritz, D. Rinck, R. Unterhinninghofen, R. Dillmann, and M. Scheuring, "Automatic segmentation of the left ventricle and computation of diagnostic parameters using region growing and a statistical model," in *Proc. of SPIE Medical Imaging*, 2005, pp. 1844–1854.
- [10] C. Lorenz and J. von Berg, "A comprehensive shape model of the heart," *Medical Image Analysis*, vol. 10, no. 4, pp. 657–670, 2006.
- [11] A. Neubauer and R. Wegenkiltl, "Analysis of four-dimensional cardiac data sets using skeleton-based segmentation," in *Proc. Int'l Conf. in Central Europe on Computer Graphics and Visualization*, 2003.
- [12] T. McInerney and D. Terzopoulos, "A dynamic finite element surface model for segmentation and tracking in multidimensional medical images with application to cardiac 4D image analysis," *Computerized Medical Imaging and Graphics*, vol. 19, no. 1, pp. 69–83, 1995.
- [13] P. Viola and M. Jones, "Rapid object detection using a boosted cascade of simple features," in *Proc. IEEE Conf. Computer Vision and Pattern Recognition*, 2001, pp. 511–518.
- [14] B. Georgescu, X.S. Zhou, D. Comaniciu, and A. Gupta, "Database-guided segmentation of anatomical structures with complex appearance," in *Proc. IEEE Conf. Computer Vision and Pattern Recognition*, 2005, pp. 429–436.
- [15] Y. Zheng, A. Barbu, B. Georgescu, M. Scheuring, and D. Comaniciu, "Fast automatic heart chamber segmentation from



ISSN: 2277-3754

International Journal of Engineering and Innovative Technology (IJET)

Volume 1, Issue 3, March 2012

3D CT data using marginal space learning and steerable features,” in Proc. Int’l Conf. Computer Vision, 2007.

- [16] Y. Zheng, B. Georgescu, A. Barbu, M. Scheuring, and D. Comaniciu, “Four-chamber heart modeling and automatic segmentation for 3D cardiac CT volumes,” in Proc. of SPIE Medical Imaging, 2008.
- [17] O. Ecabert, J. Peters, and J. Weese, “Modeling shape variability for full heart segmentation in cardiac computed-tomography images,” in Proc. of SPIE Medical Imaging, 2006, pp. 1199–1210.